Catalysis Communications 103 (2018) 24–28

Contents lists available at ScienceDirect

Catalysis Communications

journal homepage: www.elsevier.com/locate/catcom

Short communication

# $ZnO_2$-promoted ZnO as an efficient photocatalyst for the photoreduction of carbon dioxide in the presence of water

Qiangsheng Guo[a,c], Qinghong Zhang[a,*], Hongzhi Wang[b], Zhe Zhao[c,*]

[a] State key laboratory for modification of chemical fibers and polyer materials, Donghua University, Shanghai 201620, PR China
[b] College of Materials and Engineering, Donghua University, Shanghai 201620, PR China
[c] Department of Materials Science and Engineering, Shanghai Institute of Technology, Shanghai 201418, PR China

ARTICLE INFO

*Keywords:*
$ZnO_2$
ZnO
$CO_2$ phototreduction
$CH_4$
$CH_3OH$

ABSTRACT

$ZnO_2$-promoted ZnO photocatalysts were synthesized via $H_2O_2$ treatment, and their structural properties, optical properties, and activity for $CO_2$ photoreduction were systematically studied. It was revealed that an excess of $ZnO_2$ increased the surface area and enhanced oxygen vacancies, which significantly increased the adsorption capacity of molecular $CO_2$. As a result, $ZnO_2$-promoted ZnO showed a 21 times enhancement of $CO_2$ photoreduction, with the total yield of 1.0Zn-60 increased from 3.5 μmol $L^{-1}$ to 73.5 μmol $L^{-1}$ of pristine ZnO. Based on the results of in situ $CO_2$-IR and product distribution, a reaction mechanism for $CO_2$ photoreduction on ZnO catalyst was proposed.

## 1. Introduction

The increase of carbon dioxide ($CO_2$) emissions and shortage of fossil fuels induce great demand for new clean energy. In particular, it is highly attractive to seek effective approaches for efficient $CO_2$ resourcing [1]. Since the first report on photocatalytic reduction of $CO_2$ into organic compounds over suspended $TiO_2$ particles by Fujishima et al. [2], recycling $CO_2$ to fuels using sunlight as the sole energy input offered a brand new opportunity for a sustainable energy future. Various photocatalysts such as $TiO_2$ [3], $BiVO_4$ [4], $Bi_2WO_6$ [5], $Zn_2GeO_4$ [6] ZnO [7], and CdS [8,9], have been investigated for the conversion of $CO_2$ into small organic molecules for many years.

ZnO has been intensively studied as a photocatalyst due to its interesting structural characteristics and special physicochemical band [10,11]. ZnO is a typical direct band gap semiconductor, manifesting 10–100 folds higher electron mobility, and thus enhancing electron separation transfer efficiency. Undoubtedly, ZnO will widely be used in $CO_2$ photoreduction as an excellent catalyst in the next few decades. However, the efficiencies for $CO_2$ photoreduction of these ZnO-based photocatalysts are usually unsatisfactory [12,13], which might be ascribed to ZnO surface structures [14] including crystal structure, morphology, surface defects, and so on. To enhance the catalytic activity of ZnO, much effort has been made to control its structure [11,14,15], Amine-functionalized ZnO nanosheets were prepared through a hydrothermal method, which has a hydroxyl group, for covalent attachment on ZnO and the terminal amine groups on ZnO surfaces substantially increase the capability of $CO_2$ capture, resulting in effective $CO_2$ activation [14]. Surface oxygen vacancies introduced into the ZnO photocatalyst by methods such as vacuum deoxidation [16], ball milling [17], cold plasma treatment [18], and $H_2$ reduction at high temperature [19,20], can serve as photoinduced charge traps as well as adsorption sites where the charge transfer to the adsorbed species can prevent the electron-hole recombination. Clearly, controlling the oxygen vacancies and enhancing adsorption capacity of $CO_2$ is very important for obtaining a high photocatalytic activity.

Lately there has been growing interest in zinc peroxide ($ZnO_2$) semiconductor materials, which show excellent optical properties [21]. $ZnO_2$ is a useful padding widely used in photocatalysis [22,23]. In this work, the $ZnO_2$/ZnO was synthesized by using ZnO nanorods and $H_2O_2$ as raw materials. We investigated the effects of $H_2O_2$ treatment conditions on the morphology and $ZnO_2$ concentration of as-prepared $ZnO_2$/ZnO. The results of catalyst characterization and $CO_2$ photoreduction reveal that the oxygen vacancies appeared and the $CO_2$ adsorption capacity enhanced after $H_2O_2$ treatment, which eventually have a positive effect in photoreduction of $CO_2$ and $H_2O$, thus constructing excellent photo-reactivity.

## 2. Experimental

Sample preparation, characterization and photocatalytic test are shown in the Supporting information.

---

* Corresponding authors.
*E-mail addresses:* zhangqh@dhu.edu.cn (Q. Zhang), zhezhao@kth.se (Z. Zhao).

http://dx.doi.org/10.1016/j.catcom.2017.09.010
Received 15 June 2017; Received in revised form 25 August 2017; Accepted 11 September 2017

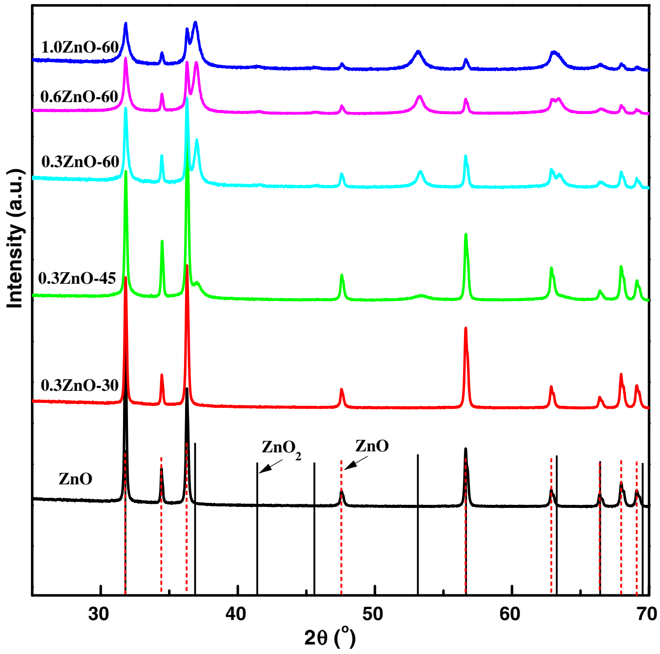

**Fig. 1.** XRD patterns pure ZnO and after $H_2O_2$ treatment at different temperature.

## 3. Results and discussion

### 3.1. Characterization of catalysts

Fig. 1 shows the XRD patterns of the as-obtained ZnO. The diffraction peaks at 31.7, 34.4, 36.2, 47.5, 56.5 and 62.8 are ascribed to the (100), (002), (101), (102), (110) and (103) planes of hexagonal ZnO (JCPDS file 89-1397) [24,25]. No additional peaks can be detected in the XRD patterns of the as-prepared ZnO nanorod. After $H_2O_2$ treatment, new peaks at 36.9 and 53.1° appear and the peak intensity continuous increase with temperature and $H_2O_2$ concertation, which correspond to the (200) and (220) crystal planes of cubic $ZnO_2$ (JCPDS file 13-311) [26] respectively. It is indicated that the starting ZnO is gradually converted into $ZnO_2$ by the $H_2O_2$ solution at a specific temperature.

Fig. S2 shows SEM images of pure ZnO and $ZnO_2$ treated by $H_2O_2$. As shown in Fig. S2a, the as-prepared ZnO exhibited typical rod-like structure with an average diameter of 60 nm. After the 0.3 mol·L$^{-1}$ $H_2O_2$ treatment at 30 °C, the nanorod morphology has little change except slightly agglomeration of a few nanorods (Fig. S2b). When the temperature was 45–60 °C, it can be noted that the some rough nanospheres emerge on the surface of ZnO nanorods, which should be attributed to $ZnO_2$ formation from ZnO reacting with $H_2O_2$. As can be seen from Fig. S2e, the nanorod was destroyed although the rod-liked structure was retained by nanoparticle stacking. Compared to the original morphology of the ZnO nanorods, numerous interconnected nanoparticles accumulate after the 1.0 mol·L$^{-1}$ $H_2O_2$ treatment at 60 °C (Fig. S2f).

To further verify the microstructure change process of ZnO after $H_2O_2$ treatment, TEM measurements were performed. Fig. 2 shows the TEM images of 0.3ZnO-60 and 0.6ZnO-60 with different magnifications. TEM images of 0.3ZnO-60 clearly show nanoparticles were grown on the surface of the nanorod and a new boundary (the white line of Fig. 2) is formed between the ZnO nanorod and generated nanoparticles. When it comes to 0.6ZnO-60, the typical rod-like structure was destroyed by the reaction between ZnO and $H_2O_2$. The original nanorods were thoroughly wrapped by accumulate nanoparticles, and formed the typical core-shell structure. It shows an obvious interface (white line in Fig. 2) between unreacted ZnO (core) and the agglomerates of nanoparticles (shell). The corresponding high-resolution TEM (HRTEM) image shows crystalline structures and a measured lattice spacing of 0.243 nm, in agreement with the d(200) spacing of $ZnO_2$. Furthermore, the SAED analysis was showed in Fig. S3. Four clear obvious rings matched to the (111), (200) and (220) planes of $ZnO_2$. These results clearly suggest that the ZnO nanorod surface were gradual eroded and $ZnO_2$ nanoparticles wrapped slowly due to the reaction of $H_2O_2$ and ZnO nanrod.

The specific surface area and pore volumes determined from the Brunauer-Emmett-Teller (BET) isotherms are summarized in Table S1. The surface areas and pore volume of ZnO were 7.26 m$^2$ g$^{-1}$ and 0.038 cm$^3$ g$^{-1}$, respectively. Obviously, the values of the surface areas and pore volume significantly increase with the increase of treatment temperature and $H_2O_2$ concentration. Combined with the above characterization of XRD and SEM, it indicates the generated $ZnO_2$ nanoparticles on the surface of the ZnO nanorod distinctly enhance the surface and pores volumes.

To gain more insight into the oxygen vacancies in the ZnO samples, the chemical states of oxygen were investigated by XPS, and the XPS spectra for O.1s are shown in Fig. 3A. The low binding energy component located at 529.4 eV ($O_I$) is attributed to the $O^{2-}$ ions in the wurtzite structure of a hexagonal $Zn^{2+}$ ion array [27]. The highest binding energy component located at 532.1 eV ($O_{III}$) can be attributed to hydroxide ($OH^-$), or peroxide ($O_2{}^{2-}$) [28]. The medium binding energy component, centered at 530.8 ($O_{II}$), is associated with $O^{2-}$ in the oxygen deficient regions with the matrix of ZnO [29]. It is believed that the intensity of this peak is connected to the variations in the concentration of oxygen states. For all ZnO samples, the surface oxygen-related chemical states were fixed and exhibited a clearly main peak of $O_I$. As shown in Table S2, the intensity of the $O_I$ peak decreased with increasing treatment temperature and $H_2O_2$ concentration, while the area ratio of $O_{II}$ peak and $O_{III}$ peak increase gradually. It suggests that the oxygen deficient and hydroxide OH/peroxide $O_2{}^{2-}$ was increased when treated with a high temperature and $H_2O_2$ concentration. When the treatment temperature is 60 °C and $H_2O_2$ concentration is 1.0 molL$^{-1}$, the oxygen deficient and peroxide $O_2{}^{2-}$ ratio increase to 41.4 and 27.3%.

Fig. 3B shows in situ DRIFT spectra obtained after $CO_2$ adsorption on modified catalysts at 325 K. A number of IR bands in the range of 1800–1000 cm$^{-1}$ are observed, and these bands are mainly due to various types of carbonate-like species including carboxylate species ($HCOO^-$), bicarbonate ($HCO_3{}^-$), mono- and bidentate-carbonate (m-$CO_3{}^{2-}$ and b-$CO_3{}^{2-}$).

The b-$CO_3{}^{2-}$ species (1608 cm$^{-1}$) and $HCO_3{}^-$ species (1495 cm$^{-1}$) are observed on the surface of unpretreated ZnO in spite of weak adsorption intensity. Comparison of the IR features of unpretreated ZnO and $H_2O_2$ treated ZnO clearly exhibit stronger b-$CO_3{}^{2-}$ species (1608 cm$^{-1}$) and $HCO_3{}^-$ species. It was found that the b-$CO_3{}^{2-}$ species were rapidly enhanced on the surface of 0.3 M-45, and slightly increased with $H_2O_2$ treatment. Meanwhile, the $HCO_3{}^-$ species continuously improve with $H_2O_2$ treatment, especially for 1.0ZnO-60 samples. Obviously, the increased velocity of b-$CO_3{}^{2-}$ species is different with $HCO_3{}^-$ species. The b-$CO_3{}^{2-}$ species is increased rapidly after $H_2O_2$ treatment at low temperature and concertation, while HCO3– species increased rapidly after $H_2O_2$ treatment at high temperature and concertation. The result suggests that the product of $ZnO_2$ after the $H_2O_2$ treatment could provide additional adsorption sites to absorb $CO_2$ and affect the chemical bonding of adsorbed $CO_2$.

### 3.2. Catalytic activity

To demonstrate the photocatalytic performance of the $ZnO_2$-promoted ZnO, photoreduction experiments of $CO_2$ with $H_2O$ under simulated solar irradiation were carried out, with the results as shown in Fig. 4. Pristine ZnO exhibited a very low photocatalytic activity, with a $CH_4$ yield at 2.6 μmol g$^{-1}$, $CH_3OH$ yield at 0.9 μmol g$^{-1}$and